Proceedings of the Sixth International Conference on
Railway Technology: Research, Development and Maintenance
Edited by: J. Pombo
Civil-Comp Conferences, Volume 7, Paper 17.4
Civil-Comp Press, Edinburgh, United Kingdom, 2024
ISSN: 2753-3239, doi: 10.4203/ccc.7.17.4
©Civil-Comp Ltd, Edinburgh, UK, 2024

Response Amplification at Railway Transition Zones - Comparison of Soft-to-Stiff and Stiff-to-Soft Transitions

A. B. Fărăgău, A. V. Metrikine and K. N. van Dalen

Faculty of Civil Engineering and Geosciences, Delft University of Technology, Netherlands

Abstract

Transition zones, characterized by significant variation in track properties (e.g., foundation stiffness) near rigid structures like bridges and tunnels, necessitate more frequent maintenance compared to standard track sections due to higher levels of differential settlements observed at transition zones. Field measurements on one-way tracks reveal asymmetric settlement patterns (i.e., different settlement in the soft-to-stiff vs stiff-to-soft transitions), yet existing literature often investigate either one or the other transition type without investigating the potential limited validity of results. This study investigates the similar aspects as well as the dissimilar ones regarding the behaviour of soft-to-stiff and stiff-to-soft transitions. Modelling results show that the behaviour of the two transition can be considerably different. These results strongly suggest that for a mitigation measure to be efficient, it may be necessary to have different designs for the two types of transition wherever possible (i.e., in one-way tracks). This study can help researchers and engineers understand the different degradation patterns obtained using more complex models or from field measurements.

Keywords: moving-load dynamics, railway transition zones, types of transition zones, direction of movement, wave propagation, differential settlements

1 Introduction

The increased demand on railway transport causes an acceleration in infrastructure degradation leading to an increased frequency of maintenance and repair operations. Transition zones, areas with substantial variation of track properties (e.g., foundation stiffness) encountered near rigid structures such as bridges, tunnels, etc. require considerably more frequent maintenance than the regular parts of the railway track [1]. This is caused by excessive differential settlements that can be related to stresses amplification encountered at transition zones [2–13]. For example, Nielsen et al. [14] found a strong correlation between the track stiffness inhomogeneity and local irregularities in the vertical track geometry (i.e., differential settlement).

Field measurements (e.g., [15]) and numerical simulations (e.g., [16]) on one-way tracks reveal a strongly asymmetric settlement pattern in the soft-to-stiff vs stiff-to-soft transitions. Despite this, the majority of literature studies of transition zones and corresponding countermeasures consider either one or the other transition type without investigating if the results are valid for both transition types. Furthermore, a limited amount of studies (e.g. [17–19]) that treat the difference between these two transition types are available in literature. However, these limited studies focus only on quantitative analysis of the response and its variation as changes are made to the structure. Currently, there is no clear explanation as to why and under which conditions the response amplification is different for the two transition types.

To this end, this study aims to explain and reveal similarities and dissimilarities in behaviour of the (i) soft-to-stiff and (ii) stiff-to-soft transitions. This study is based on work presented by the first author's PhD dissertation [20]. This study can help researchers and engineers understand the different degradation patterns obtained using more complex models or from field measurements.

2 Model formulation and solution

To investigate the responses in the soft-to-stiff and stiff-to-soft transitions, we choose one of the simplest representations of a railway track, namely an infinite Euler-Bernoulli beam resting on Winkler foundation acted upon by a moving constant load (Fig. 1). The Winkler foundation has a jump in stiffness at $x = x_{\mathrm{tc}}$ (subscript tc stands for transition centre), dividing the infinite inhomogeneous domain into two semi-infinite homogeneous ones. The equation of motion of the system reads

$$EIw'''' + \rho\ddot{w} + k_{\mathrm{d}}(x)w = -F_0\,\delta(x - vt), \qquad \forall x, \forall t, \tag{1}$$

$$w(x,t) = \begin{cases} w_{\mathrm{l}}(x,t), & x \leq x_{\mathrm{tc}}, \\ w_{\mathrm{r}}(x,t), & x \geq x_{\mathrm{tc}}, \end{cases} \qquad k_{\mathrm{d}}(x) = \begin{cases} k_{\mathrm{d,l}}, & x < x_{\mathrm{tc}}, \\ k_{\mathrm{d,r}}, & x \geq x_{\mathrm{tc}}, \end{cases}$$

where the primes and overdots represent partial derivatives with respect to space and time, respectively, EI and ρ are the bending stiffness and mass per unit length of the

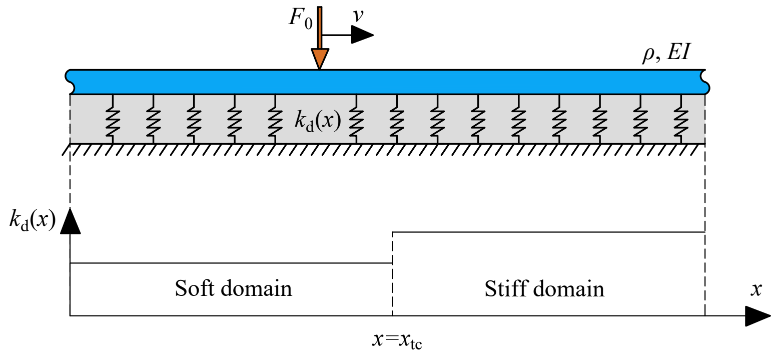

Figure 1: Model schematics: infinite Euler–Bernoulli beam resting on a piecewise-homogeneous Winkler foundation, subject to a moving constant load.

beam, respectively, while $k_{\mathrm{d,l}}$ and $k_{\mathrm{d,r}}$ are the (homogeneous) foundation stiffnesses of the left and right semi-infinite domains, respectively. F_0 and v are the magnitude and the velocity of the moving load, while w_l and w_r represent the displacements of the left and right semi-infinite domains, respectively. The space and time dependency of the unknown displacements is omitted from most expressions for brevity. Furthermore, the use of both the $\leq$ and $\geq$ signs in the definition of $w(x,t)$ emphasizes that there is continuity in this quantity at the interface between the two domains (see below).

For some results, viscous foundation damping is incorporated by an additional term $(+c_\mathrm{d}\dot{w})$ in Eq. 1, where the viscous damping coefficient c_d is given by a damping ratio ζ, which is defined similarly to that of a single-degree-of-freedom system, and reads

$$c_\mathrm{d}(x) = 2\zeta\sqrt{\rho\, k_\mathrm{d}(x)}. \tag{2}$$

As can be seen, the damping coefficient $c_\mathrm{d}(x)$ in the two domains is chosen such that the damping ratio ζ is kept constant.

At the interface between the two domains, continuity in displacement and slope as well as in shear force and bending moment is imposed. Furthermore, the displacements at infinite distance from the moving load should not be infinite (if material damping is neglected) or zero (if material damping is accounted for). The interface and boundary conditions thus read

$$w_\mathrm{l}(x_\mathrm{tc},t) = w_\mathrm{r}(x_\mathrm{tc},t), \qquad w_\mathrm{l}'(x_\mathrm{tc},t) = w_\mathrm{r}'(x_\mathrm{tc},t), \tag{3}$$

$$w_\mathrm{l}''(x_\mathrm{tc},t) = w_\mathrm{r}''(x_\mathrm{tc},t), \qquad w_\mathrm{l}'''(x_\mathrm{tc},t) = w_\mathrm{r}'''(x_\mathrm{tc},t), \tag{4}$$

$$\lim_{(x-vt)\to-\infty} w_\mathrm{l}(x,t) < \infty, \qquad \lim_{(x-vt)\to\infty} w_\mathrm{r}(x,t) < \infty. \tag{5}$$

As the system is infinite and only locally inhomogeneous, the response is assumed to be in the steady state before the load reaches the transition zone. Consequently, initial conditions do not need to be formulated. Thus, Eqs. (1) to (5) constitute a complete description of the current problem. In the next section, the steady-state solution is derived.

The response of the inhomogeneous system described by Eqs. (1)–(5) can be obtained semi-analytically in various ways (e.g., [20]), but has not been determined fully analytically yet. We choose to apply the Fourier transform over time and represent the response as a summation of wave modes because we consider this method to be most elegant for this problem. The detailed derivation of the response is presented in [20], and is omitted here for brevity. The final response reads

$$\tilde{w}(x,\omega) = \begin{cases} B_\mathrm{l}\mathrm{e}^{\mathrm{i}k_\mathrm{l}x} + C_\mathrm{l}\mathrm{e}^{k_\mathrm{l}x} + \tilde{w}_{\mathrm{p,l}}(x,\omega), & x \le x_\mathrm{tc}, \\ A_\mathrm{r}\mathrm{e}^{-\mathrm{i}k_\mathrm{r}x} + D_\mathrm{r}\mathrm{e}^{-k_\mathrm{r}x} + \tilde{w}_{\mathrm{p,r}}(x,\omega), & x \ge x_\mathrm{tc}, \end{cases} \tag{6}$$

where B_l, C_l, A_r, D_r are the free-waves amplitudes that are determined from the interface conditions $\big($Eqs. (3) and (4)$\big)$, k_l and k_r are the frequency ω dependent wavenumbers corresponding to the left/right domains, respectively, and $\tilde{w}_{\mathrm{p,l}}$, $\tilde{w}_{\mathrm{p,r}}$ are the frequency-domain particular solutions (i.e., the steady-state response) corresponding to the left/right domains, respectively. To obtain the solution in the time domain, the inverse Fourier transform is applied numerically.

3 Results

This section compares the behaviour of the two transition types from two perspectives: (i) the response (displacement, force, etc.) amplification, and (ii) the energy balance between the different system contributors (energy radiation, energy input by the load, etc.) The reason for presenting both perspectives, besides a more comprehensive investigation, is the lack of unambiguous criterion to estimate the settlement from the system response. In fact, a recent publication [21] proposes an energy criterion for this purposes, which supports the necessity of an energy analysis.

3.1 Response amplification analysis

Fig. 2 presents the transient response in the time domain together with the eigenfield (of an homogeneous system with the properties of the left domain) for comparison. Far away from the transition zone, the two responses are practically identical (theoretically they are identical only at $t \to -\infty$). When the moving load is close to the transition, the transient response is distorted in comparison to the eigenfield. In the process of the load passing the transition, waves are radiated; the most noticeable are propagating in negative x-direction, although the wave radiation occurs in both directions. Furthermore, evanescent waves that remain in the vicinity of the transition zone are also excited. It can also be observed that the wave propagation still occurs even when the load has left the transition zone (provided that the damping in the system is small).

For certain time moments, amplification of the response can be observed in the vicinity of the load, both downwards and upwards (e.g., the two middle panels in Fig.

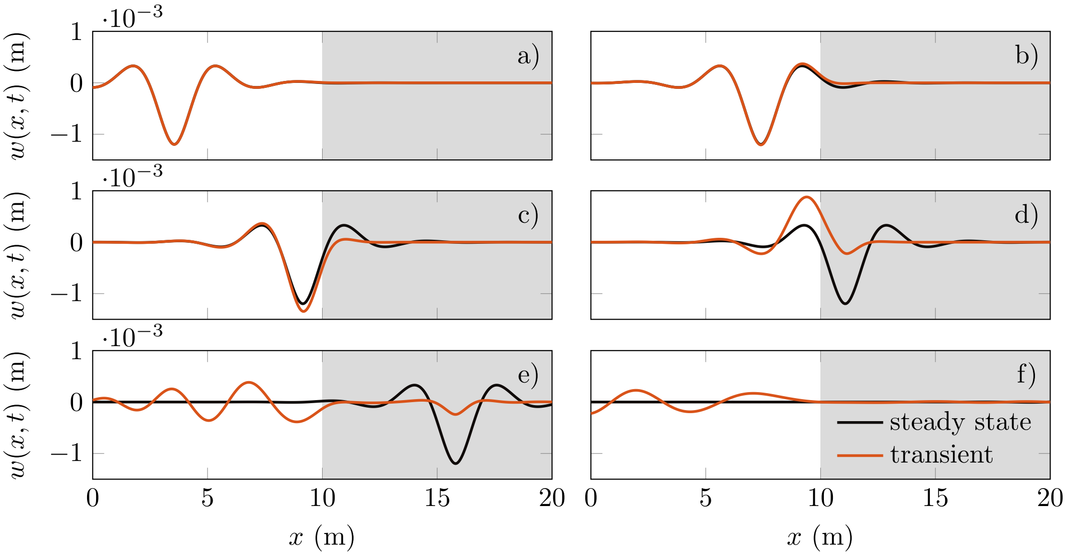

Figure 2: Snapshots of the displacement field at different time moments for the soft-to-stiff transition at a velocity of $v = 0.9c_{\text{cr}}$, where c_{cr} is the critical velocity. The stiff domain is represented through the grey background.

2). This is the amplification of stresses and strains that can be associated with the differential settlements at transition zones [7] $\big($although Fig. 2 presents displacements, the force in the foundation is obtained when multiplying the displacement by $k_{\text{d}}(x)\big)$. The response amplification is caused by the interference of the incoming eigenfield and the reflected wave-field at the transition, referred to as the *free field*. Mathematically, the free field is nothing else than the homogeneous solution $\big($see Eq. (6)$\big)$ that is necessary to satisfy the interface conditions. It becomes obvious that the more pronounced the free field is compared to the eigenfield, the larger the amplification (the amplification is always relative to the approaching eigenfield).

Fig. 3 presents a comparison of the two transition scenarios. The displacement evaluated under the moving load is presented for a relatively low velocity $v = 0.5c_{\text{cr}}$ (top panels) and a relatively high velocity $v = 0.95c_{\text{cr}}$ (top panels), where c_{cr} is the critical velocity. To highlight the response amplification, the steady-state displacement under the moving load (corresponding to the soft domain) is also presented through the horizontal dashed lines. Note that only the one in the soft domain is presented because we are interested in the response amplification before (for the soft-to-stiff) and after (for the stiff-to-soft) the man-made structure. The reason for this is that most of the differential settlement occurs in the zones adjacent to the man-made structure, and not on it [15].

Fig. 3 shows that for a relatively small load velocity, the two scenarios lead to somewhat similar results, even though the amplification in the stiff-to-soft scenario is slightly larger than in the soft-to-stiff one. More importantly, the amplification in both scenarios for the small velocity (top panels) is significantly lower compared to the large velocity (bottom panels). For the large velocity, the responses in the

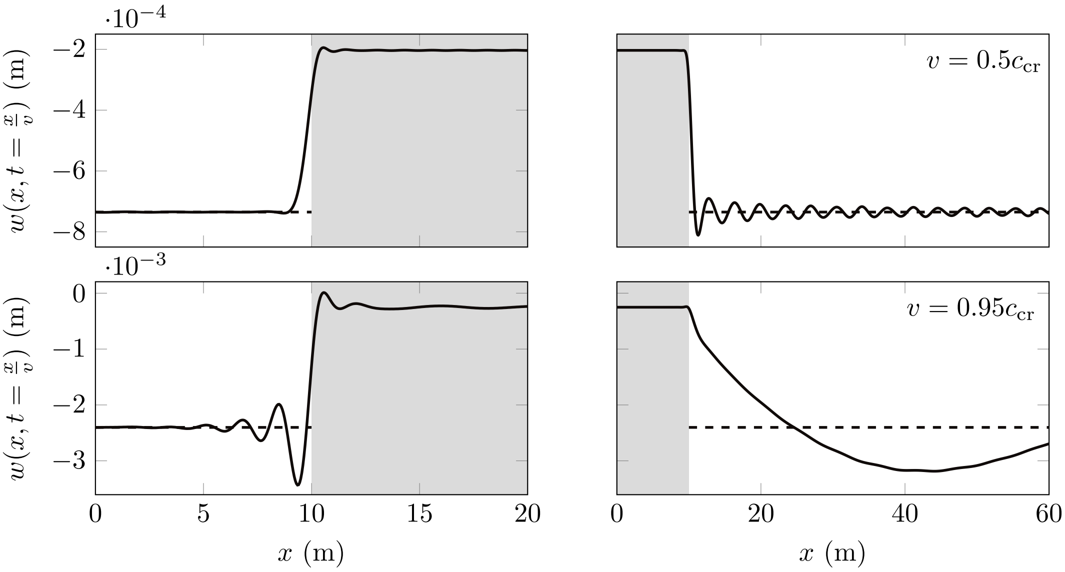

Figure 3: The transient response evaluated under the moving load in the soft-to-stiff (left panels) and stiff-to-soft (right panels) scenarios for $v = 0.5c_{\rm cr}$ (top panels) and $v = 0.95c_{\rm cr}$ (bottom panels), where $c_{\rm cr}$ is the critical velocity. The stiff domain is represented through the grey background, while the horizontal dashed lines indicate the steady-state displacement under the moving load in the soft domain.

two scenarios are significantly different. In the soft-to-stiff scenario, the eigenfield travelling in positive x-direction interferes with the free-field travelling in negative x-direction, leading to the response under the moving load to oscillate with a high frequency. In the stiff-to-soft scenario, both interfering fields (eigenfield and free field) travel in positive x-direction, and for the large speed ($v = 0.95c_{\rm cr}$), they have similar travelling velocities. This leads to their constructive interference to occur over a much larger distance, and to a low frequency oscillation of the response under the moving load. This implies that, for a relatively large velocity, the settlement in the soft-to-stiff scenario occurs close to the stiff zone and has a small wavelength, while the opposite is true for the stiff-to-soft scenario.

Fig. 3 shows that the maximum response amplification in both transition types is similar in magnitude. However, this is only the case for the system without material damping. Once damping is accounted for in the foundation, the free field decays with distance from the transition. This causes the amplification in the stiff-to-soft scenario, which occurs at a large distance from the transition, to decrease considerably even when prescribing a small amount of damping. This is shown in Fig. 4 that presents the maximum amplification in both scenarios versus relative load velocity ($v/c_{\rm cr}$), for a small (top panel) and a large (bottom panel) amount of damping. The addition of damping causes the maximum amplification in the stiff-to-soft case to decrease at large relative velocities to values even smaller than at low relative velocities, while the presence or amount of damping does not significantly influence the amplification trend

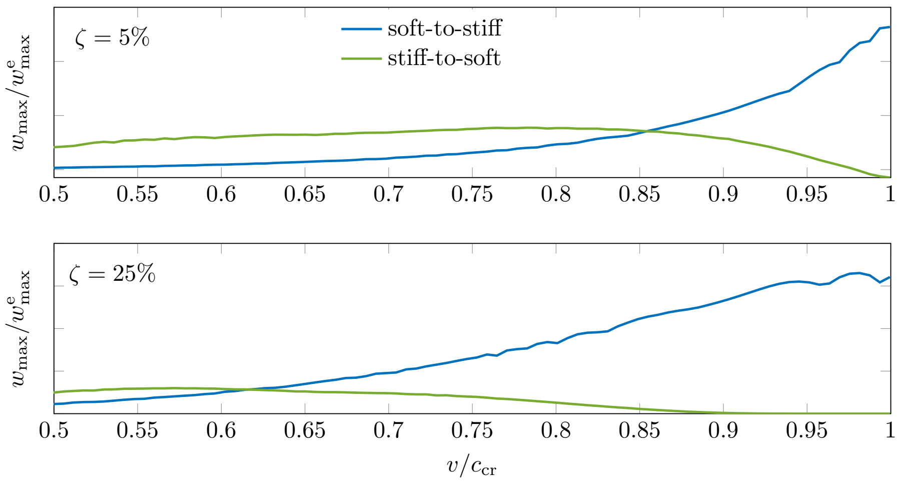

Figure 4: The maximum amplification (maximum transient response $w_{\max}$ relative to the maximum steady-state response $w^{\mathrm{e}}_{\max}$) versus velocity for a small amount (top panel) and a large amount (bottom panel) of foundation damping for both soft-to-stiff and stiff-to-soft scenarios.

in the soft-to-stiff case (it does affect the magnitude, but not the trend). It is important to note that, at low-to-medium relative velocities, the maximum amplification in the stiff-to-soft scenario can be larger than in the soft-to-stiff one, but the velocity range over which this occurs decreases the higher the damping is.

3.2 Energy analysis

The energy balance for this system has been derived in Refs. [20, 22] and for similar systems in [3], and it reads

$$E^{\mathrm{rad}} = E^{\mathrm{hf}} - \Delta W^{\mathrm{F}} - \Delta E^{\mathrm{e}}, \tag{7}$$

where E^{rad} is the energy radiation, E^{hf} is the energy introduced into the system by the horizontal force ensuring the constant velocity of the moving load (although not explicitly prescribed, this force is implicitly assumed to act on the system if a constant load velocity is imposed [3]), $\Delta W^{\mathrm{F}} = W^{\mathrm{F}}_{\mathrm{r}} - W^{\mathrm{F}}_{\mathrm{l}}$ is the work done by the vertical force, and $\Delta E^{\mathrm{e}} = E^{\mathrm{e}}_{\mathrm{r}} - E^{\mathrm{e}}_{\mathrm{l}}$ is the difference in eigenfield energy between the two domains.

Fig. 5 presents ΔE^{e} and ΔW^{F} versus relative velocity. The absolute values are presented because their sign depends on the transition type: (i) negative for soft-to-stiff, and (ii) positive for stiff-to-soft. This means that in the soft-to-stiff scenario, these quantities add to the radiated energy while in the stiff-to-soft scenario, the opposite is true. It can be seen that their qualitative behaviour with increasing velocity is similar and that the energy contained in these quantities increases considerably as the load velocity approaches the critical one.

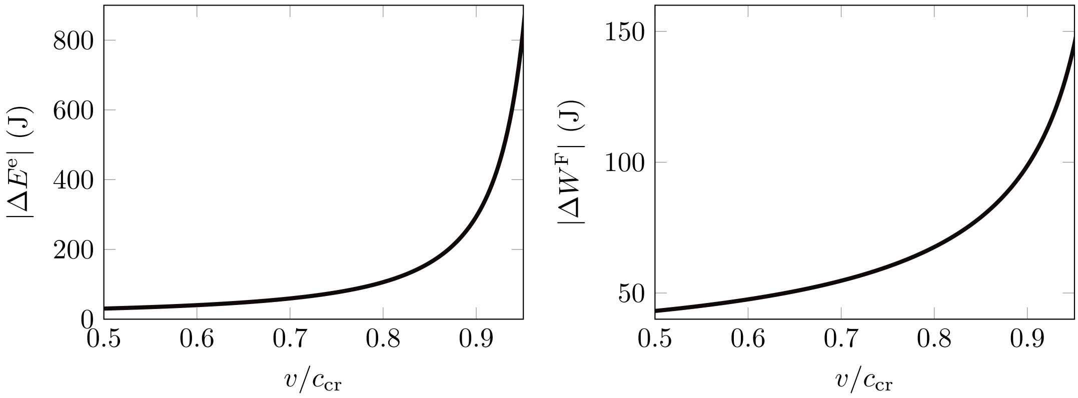

Figure 5: The absolute value of the difference in eigenfield energy ΔE^{e} and work ΔW^{F} done by the vertical load for versus relative velocity (c_{cr} corresponds to the soft domain).

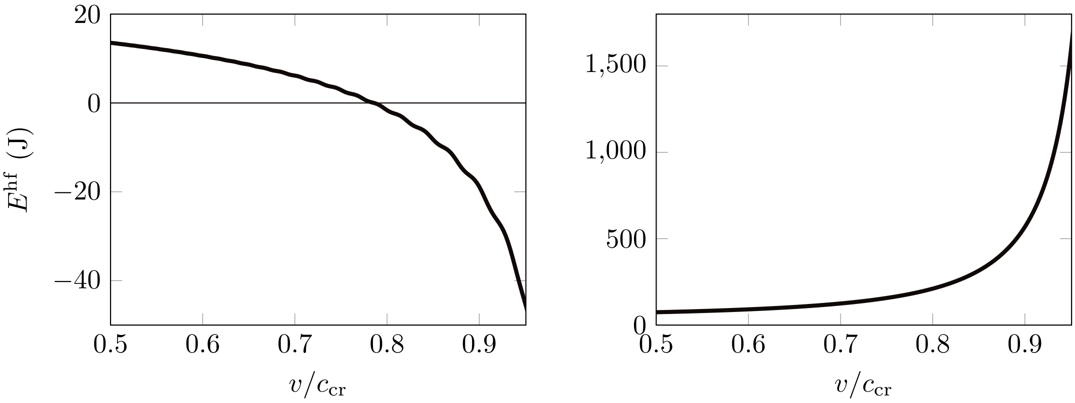

Figure 6: The energy input by the horizontal force versus load velocity for different stiffness ratios; soft-to-stiff scenario (left panel) and stiff-to-soft scenario (right panel). In the right panel, the green and red lines overlap.

Fig. 6 presents the energy input E^{hf} by the horizontal force versus relative velocity. In the soft-to-stiff scenario, the energy input for larger velocities is negative, meaning that the energy goes from the structure to the load, and not the other way around, which is, to some degree, counter intuitive. This can be explained by the fact that in the soft-to-stiff scenario, the response goes from high-energy state (soft domain) to low-energy state (stiff domain); part of the difference in eigenfield energy is radiated (transition radiation), but part goes back to the load. Fig. 6 shows that the higher the velocity, meaning a larger difference in eigenfield energy (see Fig. 5), the more energy goes back to the load. The opposite is true for the stiff-to-soft scenario where the horizontal force needs to input energy in the system to develop the high-energy eigenfield.

Fig. 7 presents the energy radiated for different load velocities. In both scenarios, the radiated energy increases significantly as the load approaches the critical velocity.

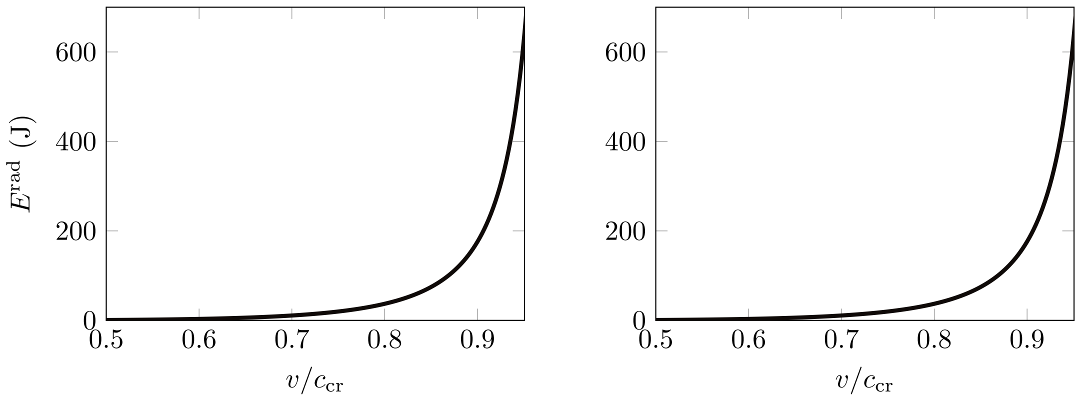

Figure 7: The energy radiated versus velocity in the soft-to-stiff (left panel) and stiff-to-soft (right panel) scenarios.

Although we do not distinguish here between energy radiated in the soft/stiff domains, the radiation in the soft zone is, in most situations, dominant (these results are omitted here for brevity) with little exceptions (see Ref. [20] for more details).

More interestingly, the energy radiation has very similar magnitudes in both the soft-to-stiff and stiff-to-soft scenarios. After a closer inspection, it seems that the total energy radiated is invariant for the two transition types. This is shown in Fig. 8 where the relative difference in radiated energy between the two scenarios (relative to the energy radiated in the soft-to-stiff scenario) is almost null; the small values are caused by numerical integration and an extremely small damping added to the foundation. This result means that the free-field propagating waves carry the same amount of energy in both scenarios. This result is unexpected, especially after showing in the time-domain analysis that the two transition types can have different behaviour.

4 Concluding remarks

This study compared the response amplification at railway transition zones for two transition types: soft-to-stiff and stiff-to-soft. The goal was to explain the difference observed in differential settlement between the two transition types, both observed in field measurements (e.g., [15]) and in numerical simulations (e.g., [16]). To this end, a simplified model of a railway track with a transition zone was formulated; more specifically, the model consists of an Euler–Bernoulli beam resting on a Winkler foundation with a piecewise-homogeneous stiffness in space, acted upon by a moving constant load.

Although the soft-to-stiff and stiff-to-soft transitions seem to poses a certain symmetry, results show that their responses are quite distinct. It was shown that the response amplification at transition zones is caused by the interference between the steady-state field (eigenfield) and the free field generated during the transition process. Results show that the difference between the two transition types stems from the

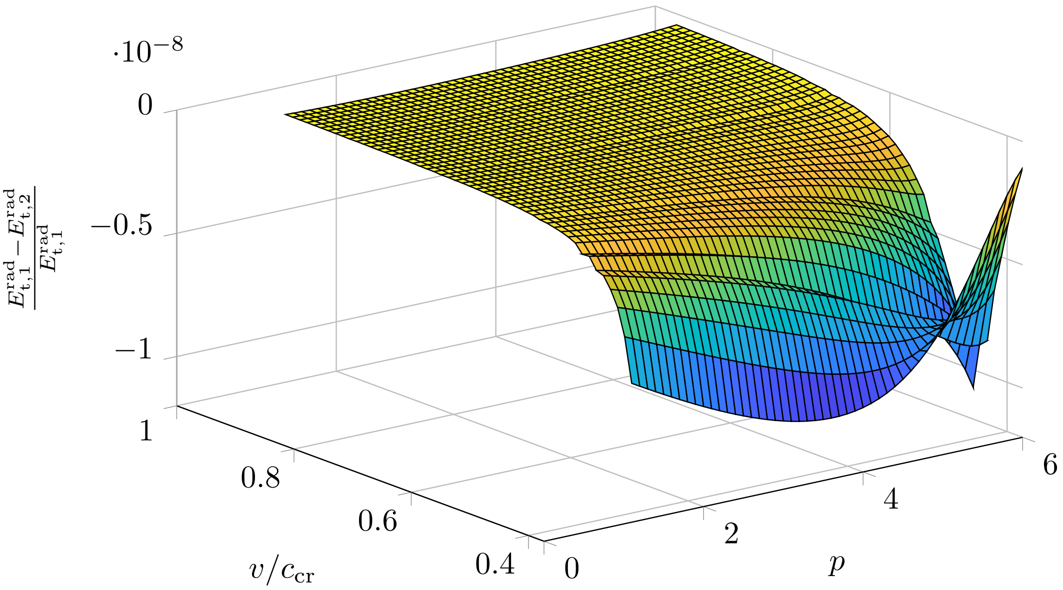

Figure 8: The relative difference in total energy radiated $E^{\mathrm{rad}}_{\mathrm{t}} = E^{\mathrm{rad}}_{\mathrm{l}} + E^{\mathrm{rad}}_{\mathrm{r}}$ between the soft-to-stiff (subscript 1) and stiff-to-soft (subscript 2) scenarios for different relative velocities and stiffness ratios. As can be seen, the relative difference is almost null.

interference between the two wave-fields:

- In the soft-to-stiff scenario, the eigenfield travelling in positive x-direction interferes with the free-field travelling in negative x-direction, leading to the response under the moving load to oscillate with a high frequency.

- In the stiff-to-soft scenario, both interfering fields (eigenfield and free field) travel in positive x-direction, and for the large speed ($v = 0.95c_{\mathrm{cr}}$), they have similar travelling velocities. This leads to their constructive interference to occur over a much larger distance, and to a low frequency oscillation of the response under the moving load.

Furthermore, the soft-to-stiff transition, the response amplification has been observed to be significant at load velocities between 75% and 100% of the critical one, and it increases considerably as the load velocity approaches the critical one. For the stiff-to-soft transition, the strongest response amplification occurs at lower velocities than for the soft-to-stiff ones, namely between 50% and 80% of the critical velocity, after which the amplification decreases. These results strongly suggests that for a mitigation measure to be efficient, it should be designed differently for the two types of transition.

Acknowledgements

This research is supported by the Dutch Technology Foundation TTW (Project 15968), part of the Netherlands Organisa- tion for Scientific Research (NWO), and which is partly funded by the Ministry of Economic Affairs of the Netherlands.

References

[1] P. Meijers, P. Hölscher, and J. Brinkman. Lasting flat raods and railways/ Literature study of knowledge and experience of transition zones. Technical report, GeoDelft, Delft, Netherlands, 2007.

[2] A. I. Vesnitskii and A. V. Metrikin. Transition radiation in One-Dimensional Elastic Systems. *Prikladnaya Mekhanika i Tekhnicheskaka Fizika*, No. 2:62–67, 1992.

[3] A. I. Vesnitskii and A. V. Metrikin. Transition radiation in mechanics. *Physics-Uspekhi*, 39(10):983–1007, 1996.

[4] K. N. van Dalen and Andrei V. Metrikine. Transition radiation of elastic waves at the interface of two elastic half-planes. *Journal of Sound and Vibration*, 310(3):702–717, 2008.

[5] Yao Shan, Bettina Albers, and Stavros A. Savidis. Influence of different transition zones on the dynamic response of track-subgrade systems. *Computers and Geotechnics*, 48:21–28, 2013.

[6] Karel N. van Dalen, Apostolos Tsouvalas, Andrei V. Metrikine, and Jeroen S. Hoving. Transition radiation excited by a surface load that moves over the interface of two elastic layers. *International Journal of Solids and Structures*, 73-74:99–112, 2015.

[7] Michaël J. M. M. Steenbergen. Physics of railroad degradation: The role of a varying dynamic stiffness and transition radiation processes. *Computers and Structures*, 124:102–111, 2013.

[8] Andrei B. Fărăgău, Andrei V. Metrikine, and Karel N. van Dalen. Transition radiation in a piecewise-linear and infinite one-dimensional structure–a Laplace transform method. *Nonlinear Dynamics*, 98:2435–2461, 2019.

[9] Andrei B. Fărăgău, Traian Mazilu, Andrei V. Metrikine, Tao Lu, and Karel N. van Dalen. Transition radiation in an infinite one-dimensional structure interacting with a moving oscillator—the Green's function method. *Journal of Sound and Vibration*, 492, 2021.

[10] André Paixão, José Nuno Varandas, and Eduardo Fortunato. Dynamic Behavior in Transition Zones and Long-Term Railway Track Performance. *Frontiers in Built Environment*, 7(March):1–16, 2021.

[11] Andrei B. Fărăgău, João M. de Oliveira Barbosa, Andrei V. Metrikine, and Karel N. van Dalen. Dynamic amplification in a periodic structure with a transition zone subject to a moving load: three different phenomena. *Mathematics and Mechanics of Solids*, (1):1–21, 2022.

[12] João Manuel de Oliveira Barbosa, Andrei B. Fărăgău, Karel N. van Dalen, and Michael Steenbergen. Modelling ballast via a non-linear lattice to assess its compaction behaviour at railway transition zones. *Journal of Sound and Vibration*, 530(April):116942, 2022.

[13] Avni Jain, Andrei V. Metrikine, Michaël J. M. M. Steenbergen, and Karel N. van Dalen. Dynamic amplifications in railway transition zones: performance evaluation of sleeper configurations using energy criterion. *Frontiers in Built Environment*, (April), 2024.

[14] Jens C.O. Nielsen, Eric G. Berggren, Anders Hammar, Fredrik Jansson, and Rikard Bolmsvik. Degradation of railway track geometry – Correlation between track stiffness gradient and differential settlement. *Proceedings of the Institution of Mechanical Engineers, Part F: Journal of Rail and Rapid Transit*, 234(1):108–119, 2020.

[15] B. Coelho, P. Hölscher, J. Priest, W. Powrie, and F. Barends. An assessment of transition zone performance. *Proceedings of the Institution of Mechanical Engineers, Part F: Journal of Rail and Rapid Transit*, 225(2):129–139, 2011.

[16] José N. Varandas, Paul Hölscher, and Manuel A.G. Silva. Settlement of ballasted track under traffic loading: Application to transition zones. *Proceedings of the Institution of Mechanical Engineers, Part F: Journal of Rail and Rapid Transit*, 228(3):242–259, 2014.

[17] Bruno Zuada Coelho, Jeffrey Priest, and Paul Hölscher. Dynamic behaviour of transition zones in soft soils during regular train traffic. *Proceedings of the Institution of Mechanical Engineers, Part F: Journal of Rail and Rapid Transit*, 232(3):645–662, 2018.

[18] Khosrow Asghari, Saeed Sotoudeh, and Jabbar Ali Zakeri. Numerical evaluation of approach slab influence on transition zone behavior in high-speed railway track. *Transportation Geotechnics*, 28(February):100519, 2021.

[19] Ilaria Grossoni, Samuel Hawksbee, Pedro Jorge, Yann Bezin, and Hugo Magalhaes. Prediction of track settlement at high-speed railway transitions between embankment and bridge in the proximity of a turnout. *Transportation Geotechnics*, 37(April):100879, 2022.

[20] Andrei B. Fărăgău. *Understanding degradation mechanisms at railway transition zones using phenomenological models*. PhD thesis, Delft University of Technology, 2023.

[21] A. Jain, A. V. Metrikine, M. J.M.M. Steenbergen, and K. N. van Dalen. Design of railway transition zones: A novel energy-based criterion. *Transportation Geotechnics*, 46(March):101223, 2024.

[22] A. R. M. Wolfert. *Wave effects in one-dimensional elastic systems interacting with moving loads*. PhD thesis, Delft University of Technology, 1999.